a given configuration in the form

$$(\tau_{est} \cdot U/L) = T(M_e, Re_L, T_w/T_o)$$

For the acoustic propagation the characteristic velocity U is the local speed of sound and L is a characteristic dimension related to the length of the interaction region through the parameter T_a. For the times to establish equilibrium of momentum and energy τ_p and τ_Q, $T_{p,Q}$ represents parameters which are related to the mixing process in the viscous shear layer and are significantly larger in fully laminar flows than in turbulent flows. Correlations of the measurements of the time required to achieve steady pressure and heat transfer levels in the base region behind the 4 spherical models over a range of freestream conditions are shown in Fig. 4. It can be seen that for the range of conditions studied the nondimensional establishment time is weakly influenced by the Mach number and Reynolds number of the freestream. The establishment time is directly proportional to the scale of the separated region and decreases with increasing freestream velocity. Because the establishment times we observe in these base flows are significantly longer than the acoustic time, we conclude that in these large separated regions the establishment of the viscous mixing is the dominant mechanism in attaining flow equilibrium. The heat transfer measurements, which take longer to stabilize, indicate that changes in the macroscopic structure of the base flow after the base pressure has stabilized do not significantly influence the gross properties of these regions. The measurements of the variation of base pressure with Reynolds number made in the present program together with earlier measurements made on spherical models, indicate the mixing process in the near wake was laminar in our studies.

The volumes of the separated regions which were studied in the work on shock-wave–boundary-layer interaction were very small in comparison to those encountered in the base flow studies and we found that the additional time required beyond the acoustic propagation time to attain flow equilibrium was small. Figure 3b shows a correlation of the measurements of time establishment nondimensionalized by the final interaction length and the acoustic propagation speed close to the wall. The experimental studies have shown that in these high temperature hypersonic flows the establishment times of separated regions depend strongly on size and geometry of the interaction regions. Whereas the time to establish the separated base flow behind a sphere is primarily dependent on the viscous mixing process to attain equilibrium, for the slender shock induced separated regions examined in our studies the establishment time can be found with good accuracy by calculating the time and pressure disturbances to traverse the entire length of the interaction region.

IV. Conclusions

Fitted with an extended driver section running times approaching 30 msec were obtained at low incident shock Mach numbers in the CAL 48 in. shock tunnel. Correlations of the measurements showed that just under 30 body lengths of flow ($t_pU/D = 27.9$) were required for the pressure in a base region to stabilize, with the heat transfer to this region taking a factor of two longer to reach equilibrium. The flow establishment time of a region of shock-wave–boundary-layer interaction could be found with good accuracy by calculating the time for an acoustic wave to traverse the total length of the interaction region, which in the present studies was less than 3 msec.

Reference

[1] Holden, M. S., "The Establishment Time of Laminar Separated Flows," Rept. 179, March 1971, Cornell Aeronautical Laboratory Inc., Buffalo, N.Y.

Thermodynamic Properties and Nozzle Flow of Hydrogen to 1000 atm and 100,000°K

R. W. Patch*
NASA Lewis Research Center, Cleveland, Ohio

Introduction

The need for reliable thermodynamic properties and nozzle-flow calculations for high-temperature hydrogen gas occurs in gaseous-core nuclear rockets and arcjets. A number of investigators have calculated high-temperature thermodynamic properties using a variety of assumptions. Rosenbaum and Levitt[1] included a covolume correction. McGee and Heller[2] included Debye-Hückel corrections. McChesney[3] pointed out that McGee and Heller were inconsistent. Krascella[4] used lowering of the ionization potential according to Ecker and Weizel,[5] who later retracted their work.[6] King[7] assumed ideal gases in his thermodynamic property and nozzle flow calculations. Thus, previous to this author's work there were no reliable Debye-Hückel thermodynamic properties or nozzle flow calculations for hydrogen.

Thermodynamic Priperties

The thermodynamic properties were based on compositions calculated by Patch.[8] In Ref. 8 the species H, H^+, e^-, H_2, H^-, H_2^+, and H_3^+ were included for conditions where each was important. Above 2000°K there was appreciable ionization, so the generally accepted Debye-Hückel approximation for charged particle interactions was used. Above 1300°K electronically excited states of H and H_2 were included, necessitating some sort of cutoff. For high degrees of ionization the perturbation of the energy levels is due principally to coulomb forces, so that one method of cutoff should be used, whereas for low degrees of ionization the perturbation of the energy levels is due principally to neutral particles, so that another method of cutoff should be used. Hence the cutoff was calculated by the Deybe-Hückel method[8] and a modified Bethe method,[9] and the method which cut off the most states was used. It was assumed that the ortho-para ratios of the ground electronic states of H_2 and H_2^+ had their equilibrium values. For high degrees of ionization it was assumed the only species were H, H^+, e^-, H^-, and H_2^+, and equilibrium

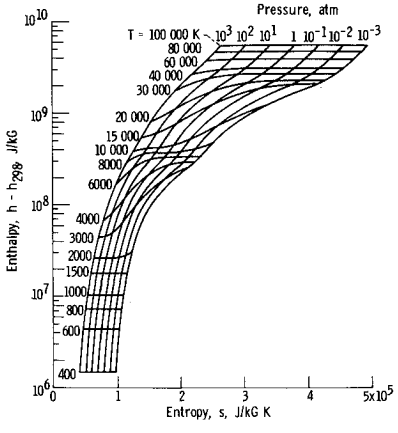

Fig. 1 Mollier diagram for hydrogen in chemical equilibrium in the Debye-Hückel approximation with equilibrium ortho-para ratio.

Received June 10, 1971.
* Research Scientist. Member AIAA.

was calculated by a major-minor Debye-Hückel iteration scheme.

The derivations of the enthalpy per unit mass h, entropy per unit mass s, and pressure p are straightforward. Each is the sum of an ideal gas term and an excess term due to coulomb interactions between free particles. The ideal gas terms are readily found from elementary statistical mechanics. The excess Helmholtz free energy, excess pressure, and excess Gibbs free energy were given in Ref. 8. The excess enthalpy and entropy follow from thermodynamic identities. Consequently

$$h = \frac{5nRT}{2\rho V} + \frac{RT^2}{\rho V}\sum_i n_i\left(\frac{\partial \ln q_i}{\partial T}\right)_V - \frac{kT\kappa^3}{6\pi\rho} \quad (1)$$

$$s = \frac{5nR}{2\rho V} + \frac{RT}{\rho V}\sum_i n_i\left(\frac{\partial \ln q_i}{\partial T}\right)_V + \frac{R}{\rho V}\sum_i n_i \ln\left[\frac{Vq_i}{N_o n_i}\left(\frac{m_i kT}{2\pi\hbar^2}\right)^{3/2}\right] - \frac{k\kappa^3}{24\pi\rho} \quad (2)$$

$$p = (nRT/V) - kT\kappa^3/(24\pi) \quad (3)$$

where n is the number of moles of all species in volume V, R is the universal gas constant, T is the absolute temperature, ρ is the density, k is the Boltzmann constant, κ is the reciprocal Debye length,[8] N_o is Avogadro's number, $\hbar$ is Planck's constant divided by 2π, and n_i, m_i, and q_i are the moles, mass, and internal partition function, respectively, of species i. All internal partition functions were taken relative to the internal energy of e^- and the gound electronic state of H. The summations over i were over all important species up to seven, depending on temperature and pressure. The specific heat at constant pressure c_p was found by numerical differentiation of h.

The isentropic exponent γ is useful in calculating sonic velocity $(\gamma p/\rho)^{1/2}$ where

$$\gamma = \left(\frac{\partial \ln p}{\partial \ln \rho}\right)_s = \frac{\rho c_p}{p\left[c_p\left(\frac{\partial \rho}{\partial p}\right)_T - \frac{T}{\rho^2}\left(\frac{\partial \rho}{\partial T}\right)_p^2\right]} \quad (4)$$

The partial derivatives of ρ were obtained by numerical differentiation.

Results are presented in a Mollier diagram (Fig. 1). Since interactions between neutral particles and between neutral and charged particles were neglected, there were errors estimated to approach 15% in the lower left corner of the Mollier diagram, but negligible elsewhere.

The Deybe-Hückel approximation is invalid beyond the critical equivalent concentration of charged particles.[10,8] However, for the conditions of Fig. 1, the equivalent concentration never exceeded 0.6 of the critical equivalent concentration. Use of the Debye-Hückel approximation instead of the ideal-gas approximation affected the thermodynamic properties, as much as 14.9% in the case of c_p. Thermodynamic properties in the form of tables (Ref. 11), punched cards, or user-supplied magnetic tape may be obtained from the author as soon as officially released.

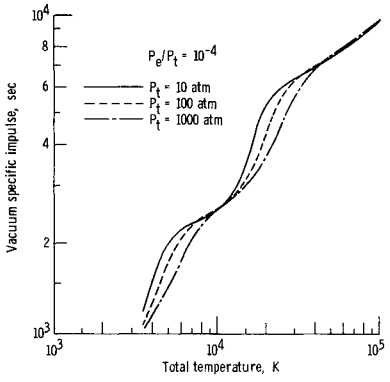

Fig. 2 Vacuum specific impulse vs total temperature for choked nozzle flow with shifting chemical equilibrium in Debye-Hückel approximation.

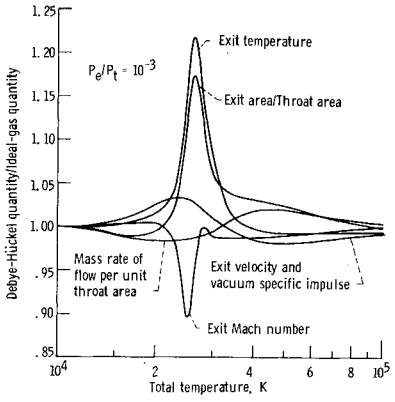

Fig. 3 Ratio of nozzle flow quantities (with leaders) calculated by two approximations vs total temperature for shifting chemical equilibrium at a total pressure of 10^3 atm.

Nozzle Flow

Calculations of choked, isentropic, one-dimensional nozzle flow with shifting chemical equilibrium are useful in predicting rocket performance. Such calculations were done using the above thermodynamic properties for hydrogen with equilibrium ortho-para ratio. Thermodynamic properties for normal hydrogen would have been more appropriate, but the resulting error was negligible. The vacuum specific impulse is given in Fig. 2, where p_t is total pressure and p_e is exit pressure. Nozzle flow tables are included in Ref. 11. Use of the Debye-Hückel approximation instead of the ideal-gas approximation had an appreciable effect on nozzle flow, as shown in Fig. 3. Effects on nozzle flow of other diatomic gases with similar ionization potential would be expected to be of the same order of magnitude.

References

[1] Rosenbaum, B. M. and Levitt, L., "Thermodynamic Properties of Hydrogen from Room Temperature to 100,000°K," TN D-1107, 1962, Cleveland, Ohio, NASA.

[2] McGee, H. A., Jr. and Heller, G., "Plasma Thermodynamics 1: Properties of Hydrogen, Helium, and Lithium as Pure Elemental Plasma," *ARS Journal*, Vol. 32, No. 2, Feb. 1962, pp. 203–215.

[3] McChesney, M., "Debye-Hückel Plasma Corrections," *AIAA Journal*, Vol. 1, No. 7, July 1963, pp. 1666–1668.

[4] Krascella, N. L., *Tables of the Composition, Opacity, and Thermodynamic Properties of Hydrogen at High Temperatures*, NASA SP-3005, 1963.

[5] Ecker, G. and Weizel, W., "Zustandssumme und effektive Ionisierungsspannung eines Atoms im Inneren des Plasmas," *Annalen der Physik (Leipzig)*, Vol. 17, No. 2-3, Feb. 1, 1956, pp. 126–140.

[6] Ecker, G. and Kröll, W., "Lowering of the Ionization Energy for a Plasma in Thermodynamic Equilibrium," *The Physics of Fluids*, Vol. 6, No. 1, Jan. 1963, pp. 62–69.

[7] King, C. R., "Compilation of Thermodynamic Properties, Transport Properties, and Theoretical Rocket Performance of Gaseous Hydrogen," TN D-275, 1960, NASA.

[8] Patch, R. W., "Absorption Coefficients for Hydrogen—I. Composition," *Journal of Quantitative Spectroscopy and Radiative Transfer*, Vol. 9, No. 1, Jan. 1969, pp. 63–87.

[9] Bond, J. W., Jr., "Structure of a Shock Front in Argon," *Physical Review*, Vol. 105, No. 6, March 15, 1957, pp. 1683–1694.

[10] Berlin, T. H. and Montroll, E. W., "On the Free Energy of a Mixture of Ions: An Extension of Kramer's Theory," *Journal of Chemical Physics*, Vol. 20, No. 1, Jan. 1952, pp. 75–84.

[11] Patch, R. W., "Thermodynamic Properties and Theoretical Rocket Performance of Hydrogen to 100,000°K and 1.01325 × 10^8 N/m^2," proposed SP, Cleveland, Ohio, NASA.